



# Synthesis of methanediol [CH<sub>2</sub>(OH)<sub>2</sub>]: The simplest geminal diol

Cheng Zhu<sup>a,b,1</sup>, N. Fabian Kleimeier<sup>a,b,1</sup> , Andrew M. Turner<sup>a,b</sup>, Santosh K. Singh<sup>a,b</sup>, Ryan C. Fortenberry<sup>c,2</sup> , and Ralf I. Kaiser<sup>a,b,2</sup> 

<sup>a</sup>Department of Chemistry, University of Hawaii at Manoa, Honolulu, HI 96822; <sup>b</sup>W. M. Keck Laboratory in Astrochemistry, University of Hawaii at Manoa, Honolulu, HI 96822; and <sup>c</sup>Department of Chemistry & Biochemistry, University of Mississippi, MS 38677

Edited by Robert Field, Chemistry, Massachusetts Institute of Technology, Cambridge, MA; received July 2, 2021; accepted November 18, 2021

**Geminal diols—organic molecules carrying two hydroxyl groups at the same carbon atom—have been recognized as key reactive intermediates by the physical (organic) chemistry and atmospheric science communities as fundamental transients in the aerosol cycle and in the atmospheric ozonolysis reaction sequence. Anticipating short lifetimes and their tendency to fragment to water plus the aldehyde or ketone, free geminal diols represent one of the most elusive classes of organic reactive intermediates. Here, we afford an exceptional glance into the preparation of the previously elusive methanediol [CH<sub>2</sub>(OH)<sub>2</sub>] transient—the simplest geminal diol—via energetic processing of low-temperature methanol–oxygen ices. Methanediol was identified in the gas phase upon sublimation via isomer-selective photoionization reflectron time-of-flight mass spectrometry combined with isotopic substitution studies. Electronic structure calculations reveal that methanediol is formed via excited state dynamics through insertion of electronically excited atomic oxygen into a carbon–hydrogen bond of the methyl group of methanol followed by stabilization in the icy matrix. The first preparation and detection of methanediol demonstrates its gas-phase stability as supported by a significant barrier hindering unimolecular decomposition to formaldehyde and water. These findings advance our perception of the fundamental chemistry and chemical bonding of geminal diols and signify their role as an efficient sink of aldehydes and ketones in atmospheric environments eventually coupling the atmospheric chemistry of geminal diols and Criegee intermediates.**

methanediol | aerosols | physical organic chemistry | photoionization | astrochemistry

Since the turn of the century, geminal diols—defined as organic molecules carrying two hydroxyl groups (OH) at the same carbon atom—have been recognized as key reactive intermediates by the physical (organic) chemistry and atmospheric science communities as fundamental transients in the aerosol cycle (1–3). However, even the simplest representative of a geminal diol—methanediol [CH<sub>2</sub>(OH)<sub>2</sub>] (**1'**, **1''**)—has not been isolated yet and is conjectured only to exist as short-lived intermediates in the troposphere and in aqueous solutions of formaldehyde (H<sub>2</sub>CO) as a transient driven by the inherent dehydration tendency and instability of the two adjacent hydroxyl groups at the same carbon atom (4–7). This classifies geminal diols as one of the least-explored classes of organic reactive intermediates.

Gas-phase electronic structure calculations predict that two conformers of methanediol [CH<sub>2</sub>(OH)<sub>2</sub>] (**1'**, **1''**) are thermodynamically favorable compared to the well-known methyl peroxide isomer (CH<sub>3</sub>OOH, **2**) by 267 kJ · mol<sup>-1</sup> and 257 kJ · mol<sup>-1</sup>, respectively; these conformers are also thermodynamically and kinetically stable toward unimolecular decomposition via dehydration to the formaldehyde–water complex (**3**), as the **1'** to **3** and **1''** to **3** reactions are endoergic by 21 and 11 kJ · mol<sup>-1</sup> and have barriers of 181 and 191 kJ · mol<sup>-1</sup>, respectively (8–11) (Fig. 1). A second decomposition mechanism of **1'**/**1''** to formic acid (HCOOH) and molecular hydrogen (H<sub>2</sub>) involves a transition

state predicted to be even 159 kJ · mol<sup>-1</sup> higher than the barrier of the dehydration mechanism (12). Consequently, methanediol [CH<sub>2</sub>(OH)<sub>2</sub>] (**1'**, **1''**) is expected to be thermodynamically and kinetically stable and hence should be detectable in the gas phase once prepared. However, envisaging the complexities of a directed gas-phase synthesis and short lifetimes of these reactive intermediates, free geminal diols signify one of the most elusive groups of organic transient molecules. This system is also attractive from the viewpoint of electronic structure theory and chemical bonding to benchmark the chemical reactivity and fundamental bond-breaking processes leading to geminal diols in extreme environments.

Here, we report the very first preparation of the previously elusive methanediol [CH<sub>2</sub>(OH)<sub>2</sub>] molecule (**1'**), along with its isomer methyl peroxide isomer (CH<sub>3</sub>OOH) (**2**), through exposure of low-temperature (5 K) methanol (CH<sub>3</sub>OH)–oxygen (O<sub>2</sub>) ices to energetic electrons (*SI Appendix, Tables S1–S4*). The isomers were unambiguously identified in the gas phase upon sublimation in the temperature-programmed desorption (TPD) phase and discriminated through isomer-selective photoionization–reflectron time-of-flight mass spectrometry together with mass shifts of their isotopically substituted counterparts. The identification of the simplest geminal diol **1'** may have far-reaching consequences for the atmospheric chemistry. Thermodynamically

## Significance

**Methanediol [CH<sub>2</sub>(OH)<sub>2</sub>] represents a pivotal atmospheric volatile organic compound and plays a fundamental role in aerosol growth. Although sought for decades, methanediol has never been identified due to the inherent dehydration tendency of two adjacent hydroxyl groups (OH) at the same carbon atom. Here, we prepare and identify methanediol via processing of low-temperature ices followed by sublimation into the gas phase. These findings open up a concept to synthesize and characterize unstable geminal diols—critical organic transients in Earth's atmosphere. The excited state dynamics of oxygen may also lead to methanediol in methanol-rich interstellar ices in cold molecular clouds, followed by sublimation in star-forming regions and prospective detection of these reactive intermediates in the gas phase by radiotelescopes.**

Author contributions: C.Z. and R.I.K. designed research; C.Z., N.F.K., A.M.T., S.K.S., and R.C.F. performed research; C.Z. and R.C.F. analyzed data; and C.Z. and R.I.K. wrote the paper.

The authors declare no competing interest.

This article is a PNAS Direct Submission.

This article is distributed under [Creative Commons Attribution-NonCommercial-NoDerivatives License 4.0 \(CC BY-NC-ND\)](https://creativecommons.org/licenses/by-nc-nd/4.0/).

<sup>1</sup>C.Z. and N.F.K. contributed equally to this work.

<sup>2</sup>To whom correspondence may be addressed. Email: r410@olemiss.edu or ralfk@hawaii.edu.

This article contains supporting information online at <http://www.pnas.org/lookup/suppl/doi:10.1073/pnas.2111938119/-DCSupplemental>.

Published December 28, 2021.

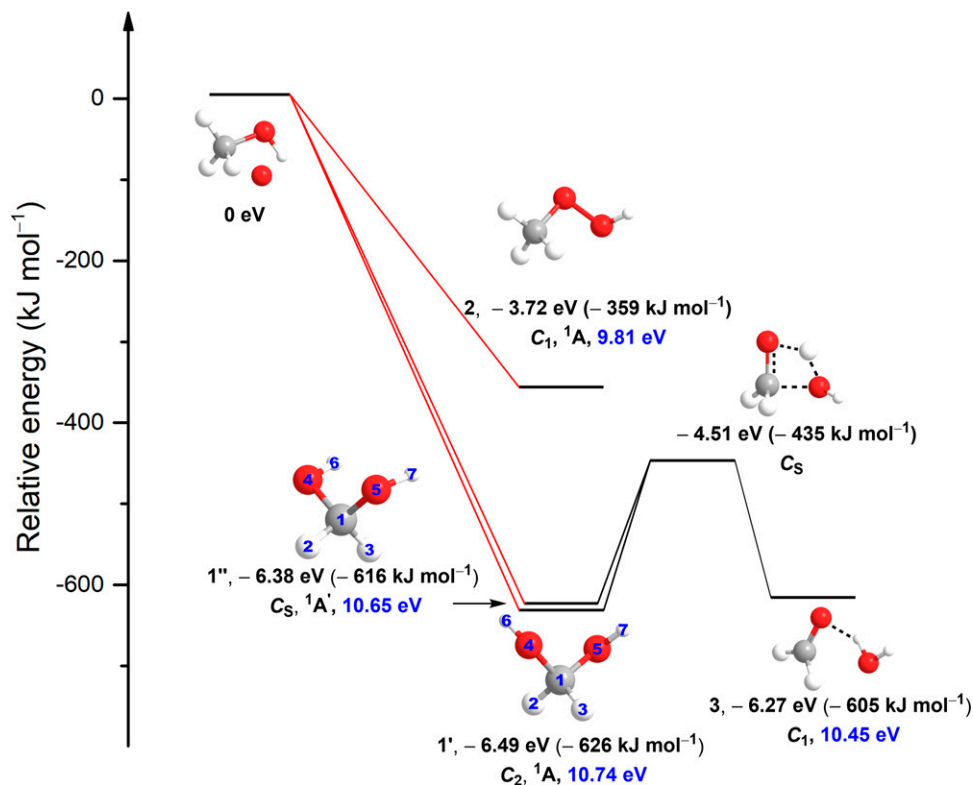


**Fig. 1.** Molecular structures of  $\text{CH}_4\text{O}_2$  isomers. Relative energies, point groups, electronic ground states, and adiabatic ionization energies (blue) of  $\text{CH}_4\text{O}_2$  isomers are also compiled. The energies were computed at the coupled cluster singles, doubles, and perturbative triples level with a complete basis set extrapolation [CCSD(T)/CBS] and include zero-point vibrational energy corrections. The atoms are color coded in gray (carbon), white (hydrogen), and red (oxygen). The formation of methanediol [ $(\text{CH}_2(\text{OH})_2$ ), **1'** and **1''**] and methyl peroxide ( $\text{CH}_3\text{OOH}$ , **2**) via excited-state oxygen atom [ $\text{O}(^1D)$ ] insertion into a carbon-hydrogen and carbon-oxygen/oxygen-hydrogen bonds of methanol ( $\text{CH}_3\text{OH}$ ), respectively, are barrierless. The transition state of the decomposition of methanediol [ $(\text{CH}_2(\text{OH})_2$ ), **1'** and **1''**] to a formaldehyde ( $\text{H}_2\text{CO}$ ) and water ( $\text{H}_2\text{O}$ ) complex ( $\text{H}_2\text{CO}\cdots\text{H}_2\text{O}$ , **3**) is also shown.

and kinetically stable geminal diols may “lock up” aldehydes and ketones—formed as byproducts of the Criegee-intermediate formation reaction—as geminal diols and hence would remove carbonyl compounds from the atmospheric ozonolysis reaction sequence (1, 13, 14). The Criegee-intermediate formation reaction is a process in which ozone reacts with alkenes forming a carbonyl oxide with two charge centers (Criegee intermediate) (14). Therefore, the existence of geminal diols and Criegee intermediates couples the chemistries of geminal diols, carbonyl compounds, and Criegee intermediates, thus helping to provide a better understanding of the atmospheric chemistry upon which all terrestrial life depends.

## Results

**Infrared Spectroscopy.** Infrared spectroscopy exploited during the irradiation phase of the ices represents an elegant tool in the identification of simple, individual molecules along with functional groups of complex organics. Since molecular oxygen is infrared inactive, the infrared spectra of the pristine ices only revealed prominent absorptions of methanol such as the O–H stretching mode ( $3,500$  to  $3,050$   $\text{cm}^{-1}$ ;  $\nu_1$ ), the C–H stretching fundamental ( $2,985$   $\text{cm}^{-1}$ ;  $\nu_2$ ), the C–H bending mode ( $1,449$   $\text{cm}^{-1}$ ;  $\nu_5$ ), and the C–O stretching mode ( $1,030$   $\text{cm}^{-1}$ ;  $\nu_8$ ) (15) (*SI Appendix, Fig. S1 and Table S2*). The radiation exposure resulted in decomposition of the precursor methanol and new absorptions at  $3,550$   $\text{cm}^{-1}$  ( $\nu_{\text{O-H}}$ ),  $2,976$   $\text{cm}^{-1}$  ( $\nu_{\text{C-H}}$ ),  $2,341$   $\text{cm}^{-1}$  ( $\text{CO}_2$ ,  $\nu_3$ ),  $2,137$   $\text{cm}^{-1}$  ( $\text{CO}$ ,  $\nu_1$ ),  $1,720$   $\text{cm}^{-1}$  ( $\nu_{\text{C=O}}$ ),  $1,500$   $\text{cm}^{-1}$  ( $\text{H}_2\text{CO}$ ,  $\nu_3$ ),  $1,378$   $\text{cm}^{-1}$  ( $\delta_{\text{C-O-H}}$ ),  $1,249$   $\text{cm}^{-1}$  ( $\text{H}_2\text{CO}$ ,  $\nu_2$ ), and  $1,075$   $\text{cm}^{-1}$  ( $\nu_{\text{C-O}}$ ) (*SI Appendix, Table S2*). The  $3,550$   $\text{cm}^{-1}$  ( $\nu_{\text{O-H}}$ ),  $1,378$   $\text{cm}^{-1}$  ( $\delta_{\text{C-O-H}}$ ), and  $1,075$   $\text{cm}^{-1}$  ( $\nu_{\text{C-O}}$ ) peaks may be associated with

methanediol, as they are close to the computed wave numbers (e.g., for **1'**, anharmonic  $\nu_{\text{O-H}} = 3,646$   $\text{cm}^{-1}$ ,  $\delta_{\text{C-O-H}} = 1,355$   $\text{cm}^{-1}$ , anti-symmetric  $\nu_{\text{C-O}} = 1,060$   $\text{cm}^{-1}$ , and symmetric  $\nu_{\text{C-O}} = 1,028$   $\text{cm}^{-1}$ ; *SI Appendix, Table S5*) and the values in a matrix isolation study by Luger et al. of ultraviolet (UV) processed methanol/ozone/argon ices ( $\nu_{\text{O-H}} = 3,639$  to  $3,638$   $\text{cm}^{-1}$  and  $3,564$   $\text{cm}^{-1}$ ,  $\delta_{\text{C-O-H}} = 1,426$  to  $1,424$   $\text{cm}^{-1}$  and  $1,359$  to  $1,354$   $\text{cm}^{-1}$ , and  $\nu_{\text{C-O}} = 1,057$  to  $1,055$   $\text{cm}^{-1}$ ) (16) as well. Isotopic experiments with  $^{13}\text{C}$ -, deuterium- (D-), and  $^{18}\text{O}$ -labeled precursors in the ices revealed red shifts of the carbon- ( $\delta_{\text{C-O-H}}$  and  $\nu_{\text{C-O}}$ ), hydrogen- ( $\nu_{\text{O-H}}$  and  $\delta_{\text{C-O-H}}$ ), and oxygen-bearing ( $\nu_{\text{O-H}}$ ,  $\delta_{\text{C-O-H}}$ , and  $\nu_{\text{C-O}}$ ) functional groups (*SI Appendix, Fig. S2 and Table S2*), respectively, thus corroborating the aforementioned assignments. However, considering the severe overlap of the absorptions of the  $\text{CH}_4\text{O}_2$  isomers/conformers with the fundamentals of the methanol and water precursors, infrared spectroscopy cannot unambiguously identify these species. Hence, an alternative analytical technique is required to identify discrete isomers selectively.

**Mass Spectrometry.** We utilized single-photon, photoionization-reflectron time-of-flight mass spectrometry (PI-ReTOF-MS) during the TPD phase of the irradiated ices to 300 K to characterize the sublimed species. This technique has a unique power to distinguish structural isomers based on their adiabatic ionization energies (IEs) by systematically adjusting the photon energy (PE) above and below the IE of the isomer(s) of interest. This approach selectively ionizes the gas-phase molecules according to their distinct IEs and examines the parent ions at a well-defined mass-to-charge ratio ( $m/z$ ). Considering the quantum chemically computed adiabatic IEs of the  $\text{CH}_4\text{O}_2$  isomers (Fig. 1), four photon

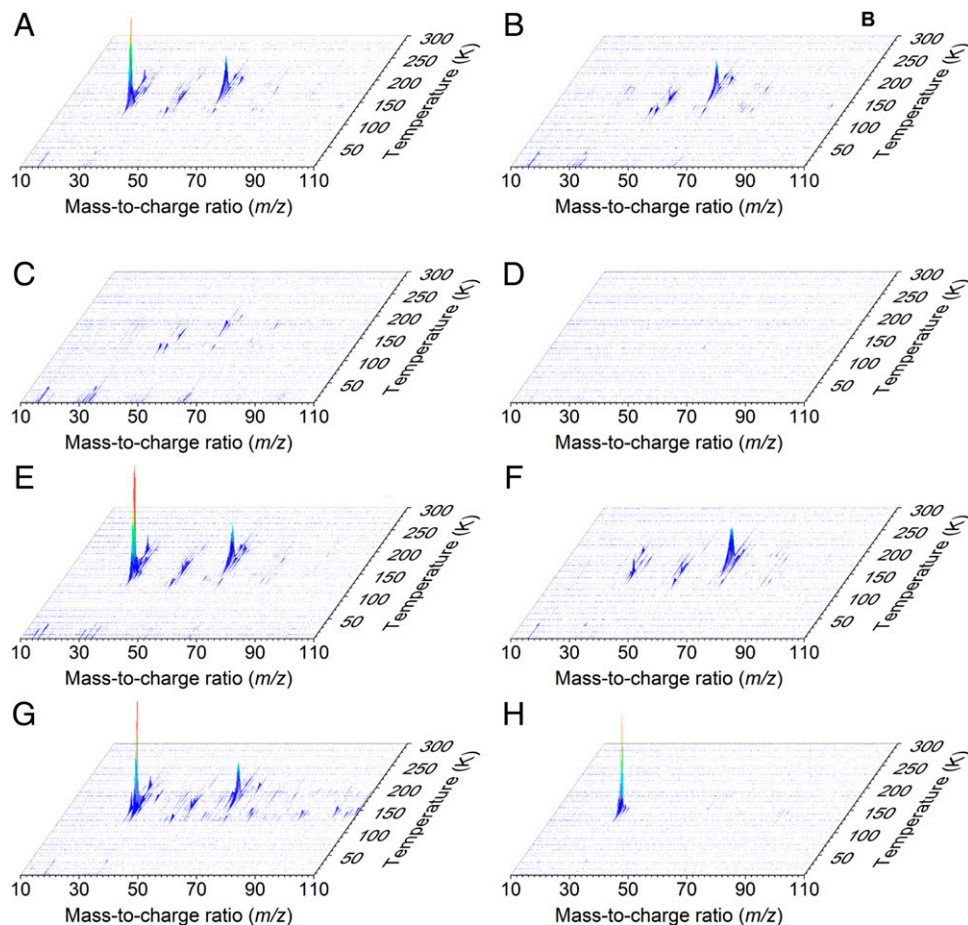


**Fig. 2.** PI-ReTOF-MS data during the TPD phase of the processed ice mixtures. (A)  $\text{CH}_3\text{OH} + \text{O}_2$ , PE = 10.86 eV; (B)  $\text{CH}_3\text{OH} + \text{O}_2$ , PE = 10.49 eV; (C)  $\text{CH}_3\text{OH} + \text{O}_2$ , PE = 10.25 eV; (D)  $\text{CH}_3\text{OH} + \text{O}_2$ , PE = 9.50 eV; (E)  $^{13}\text{CH}_3\text{OH} + \text{O}_2$ , PE = 10.86 eV; (F)  $\text{CD}_3\text{OD} + \text{O}_2$ , PE = 10.86 eV; (G)  $\text{CH}_3^{18}\text{OH} + ^{18}\text{O}_2$ , PE = 10.86 eV; and (H)  $\text{CH}_3\text{OH} + \text{O}_2$ , PE = 10.86 eV, no electron irradiation.

energies of 10.86 eV, 10.49 eV, 10.25 eV, and 9.50 eV were selected (*SI Appendix, Tables S6–S8*). Photons with energy of 10.86 eV ionize—if present—all isomers, since this PE is above the IE of each isomer (**1'** [IE = 10.66 to 10.74 eV], **1''** [IE = 10.59 to 10.65 eV], **2** [IE = 9.73 to 9.81 eV], and **3** [IE = 10.37 to 10.45 eV]). The 10.49-eV photons can photoionize only **2** and **3** but not **1'** and **1''**. The 10.25-eV photons can only ionize **2**, while 9.50-eV photons cannot ionize any isomer. Therefore, by comparing the TPD profiles of the  $\text{CH}_4\text{O}_2^+$  ions at  $m/z = 48$  at distinct PEs, **1'** and **1''** can be identified. Fig. 2 compiles the PI-ReTOF-MS data of the desorbed molecules from the irradiated ices. The extracted TPD profiles of  $m/z = 48$  ( $\text{CH}_4\text{O}_2^+$ ) are displayed in Fig. 3. At PE = 10.86 eV, three sublimation events peaking at 152 K, 162 K, and 181 K are evident (Fig. 3A). Tuning down the PE to 10.49 eV eliminates the third sublimation event at 181 K (Fig. 3B), thus providing compelling evidence that this event must be linked to the conformer pair **1'** and/or **1''** but not **2** and **3**. As the computed IEs of **1** and **3** are close to 10.49 eV, to confirm our assignments, we performed additional experiments to determine the ionization thresholds (*SI Appendix, Figs. S3–S5 and Tables S6 and S7*). The results show that the ionization threshold of **3** is  $10.44 \pm 0.01$  eV; the computed value is 10.37 to 10.45 eV. The carrier of the 181-K sublimation event has an ionization threshold of  $10.73 \pm 0.01$  eV and, therefore, can only be assigned to **1'** (computed value = 10.66 to 10.74 eV). Both low-temperature sublimation events are visible at 10.25 eV, but they vanish at PE = 9.50 eV (Fig. 3B–D). This finding suggests that these events are linked at least to **2**. Since the ratio of

the ion counts of the peaks at 152 K and 162 K is essentially identical at PE = 10.86 eV, 10.49 eV, and 10.25 eV (i.e.,  $[0.58 \pm 0.08]: 1$ ), both events likely can be associated to the same isomer **2**. The sharp peak at 152 K is connected to the cosublimation of **2** with the methanol precursor. Previous studies revealed that the sublimation of polar ices such as water (17) and methanol (15) result in a cosublimation of polar molecules, in particular those carrying hydroxyl groups, into the gas phase. It is critical to highlight that a blank experiment performed under identical conditions, but without irradiation of the ices, did not result in any ion counts at  $m/z = 48$ , demonstrating that the identified species **1'** and **2** are the result of the exposure of the ices to energetic electrons but do not originate from ion–molecule reactions in the gas phase. To provide further evidence of the identification of **1'** and **2**, three separate isotopic substitution experiments exploiting  $^{13}\text{CH}_3\text{OH} + \text{O}_2$ ,  $\text{CD}_3\text{OD} + \text{O}_2$ , and  $\text{CH}_3^{18}\text{OH} + ^{18}\text{O}_2$  ices were conducted. The TPD traces recorded in the  $\text{CH}_3\text{OH} + \text{O}_2$  system at  $m/z = 48$  were shifted 1 amu, 4 amu, and 4 amu, respectively (Fig. 4). Moreover, the TPD profiles of the isotopically substituted ices are identical to the TPD profile of  $m/z = 48$  of the  $\text{CH}_3\text{OH} + \text{O}_2$  system and essentially overlap. All together, these data indicate that the molecular carriers of these three sublimation events contain one carbon (C), four hydrogen (H), and two oxygen (O) atoms and hence can only be assigned to the molecular formula  $\text{CH}_4\text{O}_2$ . Finally, the sublimation sequence of **2** (162 K) and **1'** (181 K) is supported by an enhanced polarity of **1'**—a diol carrying two hydroxyl groups—compared to **2**—a hydroxyperoxide carrying only a single hydroxyperoxyl moiety.

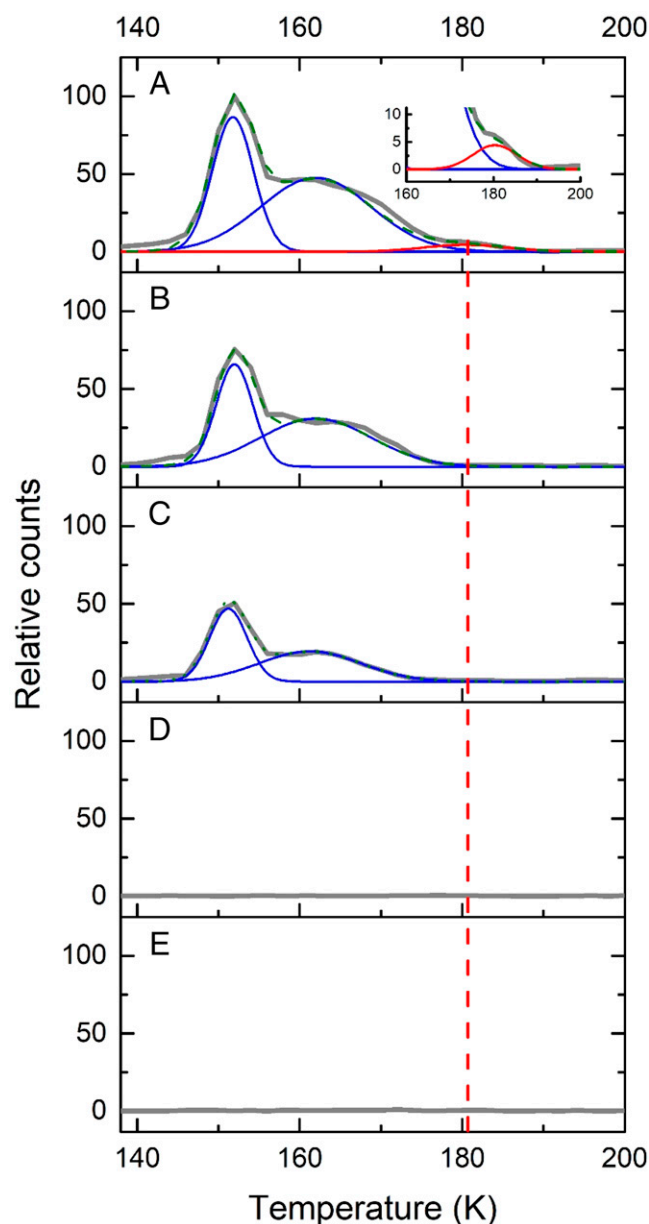


**Fig. 3.** PI-ReTOF-MS data at  $m/z = 48$  during the TPD phase of processed methanol ( $\text{CH}_3\text{OH}$ ) and oxygen ( $\text{O}_2$ ) ice mixtures. (A) PE = 10.86 eV; the inset shows the expanded view between 160 K and 200 K; (B) PE = 10.49 eV; (C) PE = 10.25 eV; (D) PE = 9.50 eV; and (E) PE = 10.86 eV, no electron irradiation.

### Discussion

With the first preparation and gas-phase identification of the geminal diol—methanediol [ $\text{CH}_2(\text{OH})_2$ ] **1'**—along with the detection of the recognized methyl peroxide isomer ( $\text{CH}_3\text{OOH}$ ) **2**, we shift our attention now to their chemical bonding and molecular structures. The conformers **1'** and **1''** have  $C_2$  and  $C_s$  symmetries, respectively. In **1'**, both hydroxyl groups are further apart than in **1''**; this leads to less steric repulsion and a thermodynamical preference of **1'** compared to **1''** by  $10 \text{ kJ} \cdot \text{mol}^{-1}$  below (Fig. 1). Under thermal equilibrium conditions at the sublimation temperatures of **1'** (about 180 K), the branching ratio of **1'** to **1''** can be estimated to be  $\sim 800$ , which supports the absence of **1''** in our experiments (*SI Appendix*). The computed C–H bond lengths in **1'** [ $\text{C}(1)\text{--H}(2) = \text{C}(1)\text{--H}(3) = 1.092 \text{ \AA}$ ; Fig. 1] are close to those in methanol ( $\text{CH}_3\text{OH}$ ) of  $\text{C--H} = 1.096 \text{ \AA}$  but longer than in methane ( $\text{CH}_4$ ,  $\text{C--H} = 1.087 \text{ \AA}$ ) due to the bond

lengthening induced by highly electronegative oxygen. The additional oxygen atom in the geminal diol results in stronger C–O bonds but weaker O–H bonds compared to methanol; this is evident from the shortening of the C–O bonds ( $1.408 \text{ \AA}$  in **1'** <  $1.427 \text{ \AA}$  in  $\text{CH}_3\text{OH}$ ) and the lengthening of the O–H bonds ( $0.964 \text{ \AA}$  in **1'** >  $0.956 \text{ \AA}$  in  $\text{CH}_3\text{OH}$ ).

We would also like to discuss potential reaction pathways involved in the formation of methanediol [ $\text{CH}_2(\text{OH})_2$ ] **1'**. Upon interaction with energetic electrons, molecular oxygen can be decomposed to two ground-state oxygen atoms  $\text{O}(^3P)$  and also to one ground state  $\text{O}(^3P)$  plus electronically excited  $\text{O}(^1D)$  (Eqs. **1a** and **1b**) (18). The Gibbs energy changes are calculated based on the Active Thermochemical Tables (11). Methanol can undergo unimolecular dissociation to the methoxy radical ( $\text{CH}_3\text{O}$ ) (Eq. **2**) or to the hydroxymethyl radical ( $\text{CH}_2\text{OH}$ ) (Eq. **3**) plus atomic hydrogen (19). Two barrierless and exoergic pathways could contribute to the formation of **1'** and **2**: oxygen atom insertion and radical–radical recombination reactions. Electronic

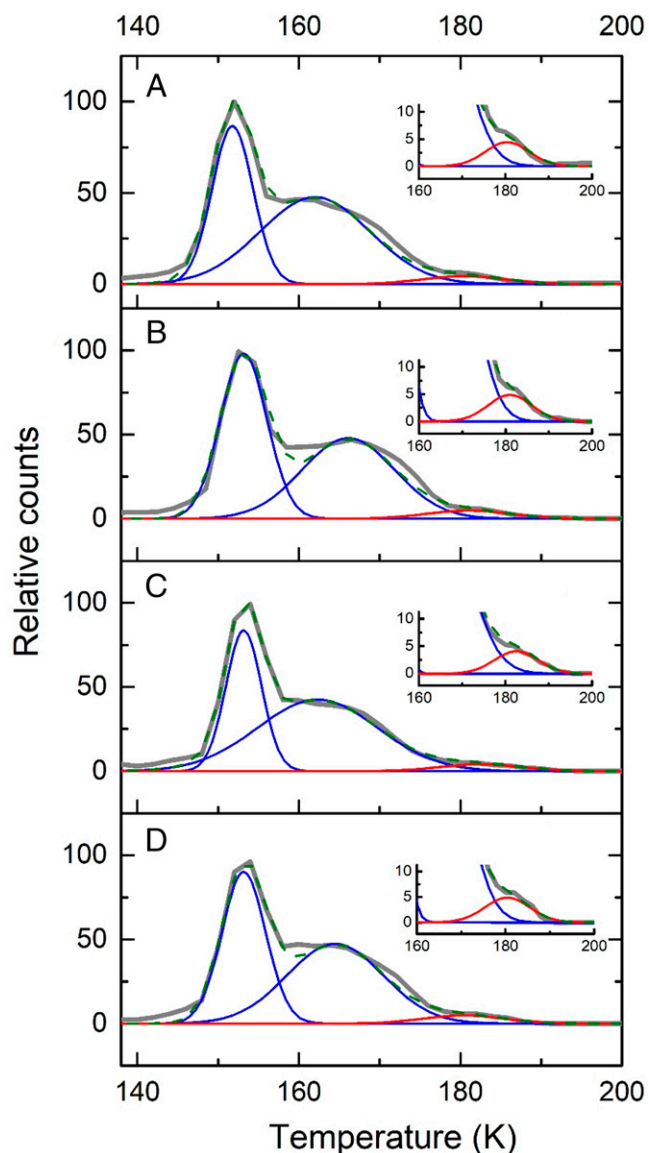
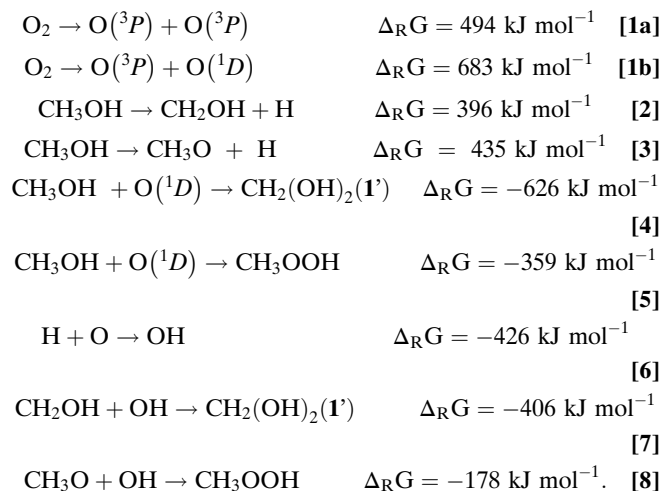


**Fig. 4.** PI-ReTOF-MS data during the TPD phase of isotopically substituted methanol ( $\text{CH}_3\text{OH}$ ) and oxygen ( $\text{O}_2$ ) ice mixtures photo ionized at a photon energy of 10.86 eV. (A)  $\text{CH}_3\text{OH} + \text{O}_2$ ,  $m/z = 48$ ; (B)  $^{13}\text{CH}_3\text{OH} + \text{O}_2$ ,  $m/z = 49$ ; (C)  $\text{CD}_3\text{OD} + \text{O}_2$ ,  $m/z = 52$ ; and (D)  $\text{CH}_3^{18}\text{OH} + ^{18}\text{O}_2$ ,  $m/z = 52$ . The inset shows the expanded view between 160 K and 200 K.

structure calculations reveal that electronically excited  $O(^1D)$  may insert barrierlessly into the C–H and C–O/O–H bonds of methanol leading to **1'** and **2**, respectively (Eqs. 4 and 5) (20, 21). The initial barrierless insertion of  $O(^1D)$  into, for example, C–H bonds has been demonstrated in elegant crossed molecular beam reactions with, for example,  $CH_4$  (22, 23). Alternatively, the oxygen atom—either ground state or electronically excited—can recombine with atomic hydrogen to the hydroxyl radical (OH) (Eq. 6) (24). If the latter holds a favorable recombination geometry with the methoxy radical ( $CH_3O$ ) or the hydroxymethyl radical ( $CH_2OH$ ), they may recombine to form **2** or **1'**, respectively, in overall exoergic Eqs. 7 and 8:



In summary, we synthesized the previously elusive methanediol molecule [ $CH_2(OH)_2$ ] **1'**—the simplest geminal diol—along with its isomer methyl peroxide ( $CH_3OOH$ , **2**) via exposure of low-temperature methanol–oxygen ices to energetic electrons. The isomers were identified explicitly during the TPD phase exploiting PI-ReTOF-MS based on a correlation of distinct ionization energies and sublimation profiles. The isotopic shifts of the parent ions in  $^{13}C$ ,  $D$ , and  $^{18}O$  substituted ices cement the molecular formula  $CH_4O_2$  for both sublimation events peaking at 162 K and 181 K. This sublimation sequence is likely the effect that the diol **1'** carries an extra OH functional group, resulting in an enhanced intermolecular potential through hydrogen bonds and, therefore, higher sublimation temperature compared to **2**. Considering the distance between the ice surface, from which the molecules are subliming in the TPD phase, and the interrogating laser beam of 2 mm along with the average velocity of **1'** of  $300 \text{ ms}^{-1}$  at 181 K, the lifetime of **1'** in the gas phase has to be at least 7  $\mu\text{s}$  to survive the flight time from the ice surface to the photoionization region, thus showing a kinetic stability of the diol **1'** in the gas phase as demonstrated by a significant barrier of  $191 \text{ kJ} \cdot \text{mol}^{-1}$  hindering unimolecular decomposition (Fig. 1).

Prior theoretical work has been devoted to exploring the stability and catalytic decomposition dynamics of **1** (8–10, 25–29). Kent et al. (9) suggested that, owing to the existence of an intramolecular hydrogen bond, tunneling of the hydroxyl proton is not expected to play a role in the decomposition of **1** to water ( $H_2O$ ) and formaldehyde ( $H_2CO$ ). However, Francisco et al. challenged this conclusion and computationally uncovered that tunneling enhances the decomposition rate by one to nine orders of

magnitude at atmospherically relevant temperatures of 200 K to 300 K (27). Tropospheric trace components such as water ( $H_2O$ ) and formic acid ( $HCOOH$ ) might lower the dehydration barrier by  $87 \text{ kJ} \cdot \text{mol}^{-1}$  to  $155 \text{ kJ} \cdot \text{mol}^{-1}$  (8, 25, 27). Furthermore, **1** may even catalyze its own decomposition at temperatures below 280 K (27). However, the ultrahigh vacuum (UHV) conditions of a few  $10^{-11}$  Torr of the studies presented here facilitate preparation and identification of **1** in an anhydrous gas phase, thus opening up the path to an experimental observation of the previously elusive, simplest geminal diol: **1**. This approach unlocks the preparation and spectroscopic studies of a previously elusive class of organic molecules—geminal diols—a group of atmospherically vital molecules previously regarded “not to exist” without the stabilization by electron pulling groups such as in chloral hydrate [ $CCl_3CH(OH)_2$ ] (30). The insertion of  $O(^1D)$  into carbon–hydrogen bonds of alcohols represents a versatile concept to prepare and to spectroscopically characterize higher homologs of **1** via reaction with  $R'CH_2OH$ , with “R” defining an alkyl group. For instance, if  $R = CH_3$ ,  $O(^1D)$  can react with ethanol ( $CH_3CH_2OH$ ) through insertion into the C–H bond of the  $CH_2$  moiety yielding the elusive 1,1-ethanediol [ $CH_3CH(OH)_2$ ];  $O(^1D)$  may also insert into a C–H bond of the methyl group forming the well-known isomer ethylene glycol ( $HOCH_2CH_2OH$ ). This identification of methanediol [ $CH_2(OH)_2$ ] **1'** along with the prospective preparations of higher-order analog geminal diols is expected to lead to a better perception of the role of benchmark organic transients in the Earth’s atmosphere.

The excited state dynamics leading to methanediol may also form methanediol in methanol-rich interstellar ices (31) on interstellar nanoparticles in cold molecular clouds by ionizing radiation (32, 33). Once formed, the transition from the molecular cloud phase to star-forming regions (33, 34), such as Sagittarius B2, leads to sublimation of the ice components so that reactive intermediates can be searched for in the gas phase by radio telescopes. The recent detection of ethanolamine ( $NH_2CH_2CH_2OH$ ) (35) in the Sagittarius B2 complex demonstrates the capability of the next generation of radio telescopes to identify exotic molecules in deep space. This offers a versatile strategy to first synthesize transient molecules, such as geminal diols, prior to their search in star-forming regions, eventually bringing us closer to an understanding of the molecular structure and chemical bonding of exotic organic molecules, which conventional wisdom suggests do not exist.

## Materials and Methods

The experiments include preparation of  $CH_3OH$  and oxygen ( $O_2$ ) ice mixtures as well as isotopically substituted counterparts ( $^{13}CH_3OH + O_2$ ,  $CD_3OD + O_2$ ,  $CH_3^{18}OH + ^{18}O_2$ ) on a low-temperature (5 K) silver wafer in a UHV chamber at base pressure of a few  $10^{-11}$  Torr (36), irradiation of the ices with energetic electrons to initiate chemical-bond cleavage processes and nonequilibrium reactions, and heating the irradiated ices from 5 K to 300 K at a rate of  $1 \text{ K} \cdot \text{min}^{-1}$  (TPD) to sublime the solid-phase species (SI Appendix, Table S1). During the irradiation and TPD phases, the ices and sublimed molecules were monitored via Fourier transform infrared spectroscopy and tunable vacuum UV PI-ReTOF-MS, respectively (SI Appendix, Tables S2–S4). Experimental and computational details are available in SI Appendix.

**Data Availability.** All study data are included in the article and/or SI Appendix.

**ACKNOWLEDGMENTS.** This work was supported by the US NSF, Division of Astronomical Sciences under Grants AST-1800975 and AST-2103269 to The University of Hawaii (R.I.K.). N.F.K. acknowledges funding from the Deutsche Forschungsgemeinschaft (German Research Foundation) for a postdoctoral fellowship (KL 3342/1-1).

- J. L. Axson, K. Takahashi, D. O. De Haan, V. Vaida, Gas-phase water-mediated equilibrium between methylglyoxal and its geminal diol. *Proc. Natl. Acad. Sci. U.S.A.* **107**, 6687–6692 (2010).
- M. K. Hazra, J. S. Francisco, A. Sinha, Hydrolysis of glyoxal in water-restricted environments: Formation of organic aerosol precursors through formic acid catalysis. *J. Phys. Chem. A* **118**, 4095–4105 (2014).
- B. Franco et al., Ubiquitous atmospheric production of organic acids mediated by cloud droplets. *Nature* **593**, 233–237 (2021).

- J. Walker, *Formaldehyde* (Reinhold, New York, 1964).
- J. Winkelman, M. Ottens, A. Beenackers, The kinetics of the dehydration of methylene glycol. *Chem. Eng. Sci.* **55**, 2065–2071 (2000).
- J. Winkelman, O. Voorwinde, M. Ottens, A. Beenackers, L. Janssen, Kinetics and chemical equilibrium of the hydration of formaldehyde. *Chem. Eng. Sci.* **57**, 4067–4076 (2002).
- N. Matubayasi, S. Morooka, M. Nakahara, H. Takahashi, Chemical equilibrium of formaldehyde and methanediol in hot water: Free-energy analysis of the solvent effect. *J. Mol. Liq.* **134**, 58–63 (2007).

8. S. Böhm, D. Antipova, J. Kuthan, Methanediol decomposition mechanisms: A study considering various ab initio approaches. *Int. J. Quantum Chem.* **58**, 47–55 (1996).
9. D. R. Kent, IV, S. L. Widicus, G. A. Blake, W. A. Goddard, III, A theoretical study of the conversion of gas phase methanediol to formaldehyde. *J. Chem. Phys.* **119**, 5117–5120 (2003).
10. M. Kumar, J. S. Francisco, The role of catalysis in alkanediol decomposition: Implications for general detection of alkanediols and their formation in the atmosphere. *J. Phys. Chem. A* **119**, 9821–9833 (2015).
11. B. Ruscic, D. H. Bross, Active Thermochemical Tables (ATcT) values based on ver. 1.122g of the thermochemical network. (Argonne National Laboratory, 2019).
12. J. S. Francisco, I. H. Williams, Reaction pathways for gas-phase hydrolysis of formyl compounds HXCO (X= H, F, and Cl). *J. Am. Chem. Soc.* **115**, 3746–3751 (1993).
13. O. Welz *et al.*, Direct kinetic measurements of Criegee intermediate (CH<sub>2</sub>OO) formed by reaction of CH<sub>2</sub>I with O<sub>2</sub>. *Science* **335**, 204–207 (2012).
14. M. I. Lester, S. J. Klippenstein, Unimolecular decay of Criegee intermediates to OH radical products: Prompt and thermal decay processes. *Acc. Chem. Res.* **51**, 978–985 (2018).
15. S. Maity, R. I. Kaiser, B. M. Jones, Formation of complex organic molecules in methanol and methanol-carbon monoxide ices exposed to ionizing radiation—A combined FTIR and reflectron time-of-flight mass spectrometry study. *Phys. Chem. Chem. Phys.* **17**, 3081–3114 (2015).
16. C. Lugez, A. Schriver, R. Levant, L. Schriver-Mazzuoli, A matrix-isolation infrared spectroscopic study of the reactions of methane and methanol with ozone. *Chem. Phys.* **181**, 129–146 (1994).
17. Y. Layssac, A. Gutiérrez-Quintanilla, T. Chiavassa, F. Duvernay, Detection of glyceraldehyde and glycerol in VUV processed interstellar ice analogues containing formaldehyde: A general formation route for sugars and polyols. *Mon. Not. R. Astron. Soc.* **496**, 5292–5307 (2020).
18. P. Cosby, Electron-impact dissociation of oxygen. *J. Chem. Phys.* **98**, 9560–9569 (1993).
19. C. J. Bennett, S.-H. Chen, B.-J. Sun, A. H. Chang, R. I. Kaiser, Mechanistical studies on the irradiation of methanol in extraterrestrial ices. *Astrophys. J.* **660**, 1588 (2007).
20. C.-K. Huang *et al.*, Dynamics of the reactions of O(<sup>1</sup>D) with CD<sub>3</sub>OH and CH<sub>3</sub>OD studied with time-resolved Fourier-transform IR spectroscopy. *J. Chem. Phys.* **137**, 164307 (2012).
21. B. M. Hays, S. L. Widicus Weaver, Theoretical examination of O(<sup>1</sup>D) insertion reactions to form methanediol, methoxymethanol, and aminomethanol. *J. Phys. Chem. A* **117**, 7142–7148 (2013).
22. X. Yang, Multiple channel dynamics in the O(<sup>1</sup>D) reaction with alkanes. *Phys. Chem. Chem. Phys.* **8**, 205–215 (2006).
23. H. Pan, K. Liu, A. Caracciolo, P. Casavecchia, Crossed beam polyatomic reaction dynamics: Recent advances and new insights. *Chem. Soc. Rev.* **46**, 7517–7547 (2017).
24. K. Hiraoka, T. Miyagoshi, T. Takayama, K. Yamamoto, Y. Kihara, Gas-grain processes for the formation of CH<sub>4</sub> and H<sub>2</sub>O: Reactions of H atoms with C, O, and CO in the solid phase at 12 K. *Astrophys. J.* **498**, 710 (1998).
25. Z. C. Kramer, K. Takahashi, V. Vaida, R. T. Skodje, Will water act as a photocatalyst for cluster phase chemical reactions? Vibrational overtone-induced dehydration reaction of methanediol. *J. Chem. Phys.* **136**, 164302 (2012).
26. S. Inaba, Theoretical study of decomposition of methanediol in aqueous solution. *J. Phys. Chem. A* **119**, 5816–5825 (2015).
27. M. Kumar, J. M. Anglada, J. S. Francisco, Role of proton tunneling and metal-free organocatalysis in the decomposition of methanediol: A theoretical study. *J. Phys. Chem. A* **121**, 4318–4325 (2017).
28. A. Parandaman, M. Kumar, J. S. Francisco, A. Sinha, Organic acid formation from the atmospheric oxidation of gem diols: Reaction mechanism, energetics, and rates. *J. Phys. Chem. A* **122**, 6266–6276 (2018).
29. G. Pitsevich, A. Y. Malevich, V. Sapeshko, The hydroxyl groups internal rotations in a methanediol molecule. *J. Mol. Spectrosc.* **360**, 31–38 (2019).
30. D. McGreer, R. Stewart, M. Mocek, The hydrates of fluoral. *Can. J. Chem.* **41**, 1024–1027 (1963).
31. A. G. G. M. Tielens, L. J. Allamandola, “Cool interstellar physics and chemistry” in *Physics and Chemistry at Low Temperatures*, L. Khriachtchev, Ed. (Jenny Stanford Publishing, 2011), pp. 341–380.
32. A. G. G. M. Tielens, Interstellar polycyclic aromatic hydrocarbon molecules. *Annu. Rev. Astron. Astrophys.* **46**, 289–337 (2008).
33. A. G. G. M. Tielens, The molecular universe. *Rev. Mod. Phys.* **85**, 1021 (2013).
34. A. G. Tielens, S. B. Charnley, Circumstellar and interstellar synthesis of organic molecules. *Orig. Life Evol. Biosph.* **27**, 23–51 (1997).
35. V. M. Rivilla *et al.*, Discovery in space of ethanalamine, the simplest phospholipid head group. *Proc. Natl. Acad. Sci. U.S.A.* **118**, e2101314118 (2021).
36. B. M. Jones, R. I. Kaiser, Application of reflectron time-of-flight mass spectrometry in the analysis of astrophysically relevant ices exposed to ionization radiation: Methane (CH<sub>4</sub>) and D<sub>4</sub>-methane (CD<sub>4</sub>) as a case study. *J. Phys. Chem. Lett.* **4**, 1965–1971 (2013).